Z. angew. Math. Phys. 55 (2004) 365–382
0044-2275/04/030365-18
DOI 10.1007/s00033-003-1119-7

Zeitschrift für angewandte Mathematik und Physik ZAMP

A gas-kinetic scheme for shallow–water equations with source terms

Huazhong Tang, Tao Tang and Kun Xu

Abstract. In this paper, the Kinetic Flux Vector Splitting (KFVS) scheme is extended to solving the shallow water equations with source terms. To develop a well-balanced scheme between the source term and the flow convection, the source term effect is accounted in the flux evaluation across cell interfaces. This leads to a modified gas–kinetic scheme with particular application to the shallow water equations with bottom topography. Numerical experiments show better resolution of the unsteady solution than conventional finite difference method and KFVS method with little additional cost. Moreover, some positivity properties of the gas–kinetic scheme is established.

Mathematics Subject Classification (2000). 65M93, 35L64, 76N10.

Keywords. Shallow water equations, source terms, gas–kinetic schemes.

1. Introduction

The study of wave motion in shallow water leads to a system of conservation laws. If the shallow water is over a wavy bottom, then the system will involve geometrical source terms. The one–dimensional problem is governed by the following equation:

$$\begin{cases} h_t + (hu)_x = 0, \\ (hu)_t + (hu^2 + \frac{1}{2}Gh^2)_x = -Gha'(x), \end{cases} \tag{1.1}$$

where G is the gravitational constant, h is the height of the water above the wavy bottom characterized by the function $a(x)$ and u is the velocity. In order to accurately capture the numerical solutions for the above equations, many approaches have been proposed, see, e.g., [1, 3, 4, 5, 7, 9].

For steady state solutions, the equilibria of the system (1.1) satisfy

$$hu \equiv h_- u_-, \tag{1.2}$$

$$\frac{u^2}{2} + (h + a(x))G \equiv \frac{u_-^2}{2} + (h_- + a_-)G, \tag{1.3}$$

where $h_- = \lim_{x\to-\infty} h(x) > 0$, $u_- = \lim_{x\to-\infty} u(x)$, and $a_- = \lim_{x\to-\infty} a(x) \geq 0$. If the function $a(x)$ is smooth and

$$\sup_x |a(x) - a_-| \ll 1, \tag{1.4}$$

then the above algebraic system has smoothly varying solutions with $h > 0$ and $\text{sign}(u) = \text{sign}(u_-)$. In [3], Greenberg and LeRoux noticed that the development of schemes that preserve such equilibria are desirable. They also observed that for scalar equation which can be regarded as model problem (1.1), the standard cell averaging schemes such as the Godunov or Lax–Friedrichs (LxF) schemes can not preserve such equilibria. For a general hyperbolic equations with source term,

$$W_t + F(W)_x = G(W),$$

in order to preserve the similar equilibria the flux function and the source term have to be well balanced, such as

$$F(W)_x = G(W).$$

Numerically, a well balanced finite volume method should satisfy

$$\frac{(F_{j+\frac{1}{2}} - F_{j+\frac{1}{2}})}{\Delta x} = G(W_j).$$

In order to make the above equation valid *generally*, the flux function at the cell interface has to reflect the source term effects. In [4] Jin proposed a simple numerical method for capturing the steady solution of hyperbolic systems with geometrical source terms. One application of his method is for the shallow water equations. Due to the simple nature of the shallow water equations, the source term $G(W_j)$ can be specifically formulated using the cell interface values so that the above equilibria are satisfied exactly. For more general source terms, such as the isothermal gas inside a gravitational field, LeVeque [5] designed a more general scheme by constructing an equilibrium initial condition at each time step for the Riemann solution. For the steady state calculation, this method has been successfully applied to both the shallow water equations and the isothermal gas flow in a gravitational field. In both LeVeque and Jin's methods, the schemes are nicely designed based on the requirement of preserving the equilibria for the shallow water equations.

In this work, we will design a well balanced scheme for the shallow water equations, aiming to obtain accurate approximations for both unsteady and steady flow situations. It is not easy to construct such a scheme when source terms are presented. For example, if the wary bottom a is approximated as a simple jump at a cell interface, see Fig.1, the source term effect on the fluid inside each cell is zero, but its effect on the cell interface flux has to be accounted. To solve the Riemann problem in Fig.1 is very difficult. However, a physically reliable scheme for both steady and unsteady calculations, which may also preserve the total energy (kinetic + potential) for the shallow water equations, can not avoid

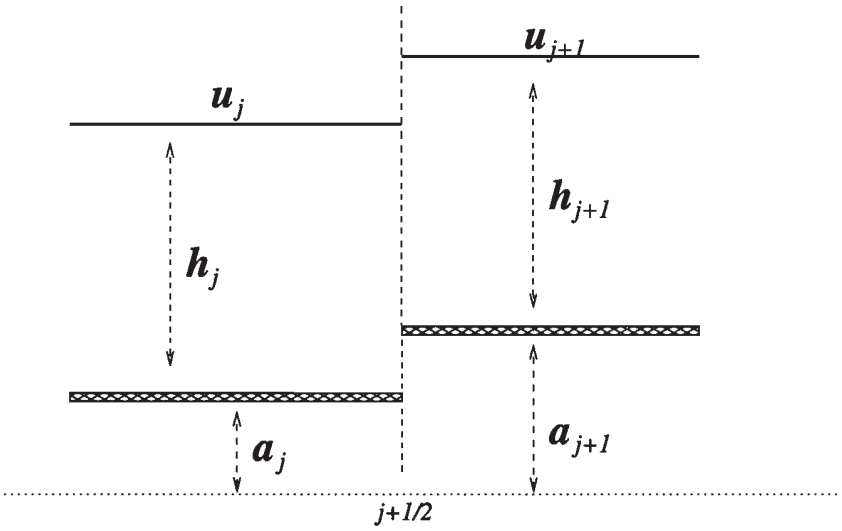

Figure 1. Riemann problem for the shallow water equations with the source term

solving such a Riemann problem. From a gas-kinetic point of view, the particles need to overcome the potential barrier $\Delta\psi = G(a_{j+1} - a_j)$ at a cell interface in order to move from one cell to another one. In other words, only these particles with enough kinetic energy can pass through the interface. For the mass flux, the number of particles leaving (receiving) from cell j through the interface $j + \frac{1}{2}$ is equal to the particles receiving (leaving) from cell $j + 1$. However, for the momentum flux, the situation is different. At the cell interface $j + \frac{1}{2}$, the momentum flux at $j + \frac{1}{2}$ for cell j is not equal to the momentum flux at $j + \frac{1}{2}$ for cell $j+1$, because the particles will get decelerated or accelerated after crossing the interface. Furthermore, some particles may be bounced back if they do not have enough kinetic energy to overcome the potential barrier. Even though the bounced particles have no contribution to the mass flux, they do have contribution to the momentum flux. The correct capturing of the source term effect on flux function not only depends on the capturing of all the above physical process happened around a cell interface, but also on the mathematical tractability to describe these process. Since the numerical formulation involved in the above process is extremely difficult, only a modified Kinetic Flux Vector Splitting (KFVS) scheme is developed in this paper. The scheme is numerically compared with the conventional KFVS scheme based on operator splitting, where the source term effect is absent in the flux evaluation.

For comparison, we briefly describe the simplest cell averaging scheme, namely the Lax–Friedrichs (LxF) scheme, for the system (1.1). A semi-explicit LxF scheme for (1.1) takes the form

$$\begin{cases} h_j^{n+1} = \dfrac{1}{2}(h_{j+1}^n + h_{j-1}^n) - \dfrac{\Delta t_n}{2\Delta x}\Big((hu)_{j+1}^n - (hu)_{j-1}^n\Big), \\ (hu)_j^{n+1} = \dfrac{1}{2}\Big((hu)_{j+1}^n + (hu)_{j-1}^n\Big) - \dfrac{\Delta t_n}{2\Delta x}\Big((hu^2 + \dfrac{1}{2}Gh^2)_{j+1}^n \\ \qquad -(hu^2 + \frac{1}{2}Gh^2)_{j-1}^n\Big) - \Delta t_n G a'(x_j) h_j^{n+1}, \end{cases} \tag{1.5}$$

where Δx and Δt_n are the mesh sizes in space and time directions respectively, and

$$h_j^n = \frac{1}{\Delta x}\int_{x_{j-1/2}}^{x_{j+1/2}} h^n(x)\, dx, \quad (hu)_j^n = \frac{1}{\Delta x}\int_{x_{j-1/2}}^{x_{j+1/2}} (hu)^n(x)\, dx, \tag{1.6}$$

where $x_{j+1/2} = (j+1/2)\Delta x$. The CFL condition is

$$\frac{\Delta t_n}{\Delta x} = \frac{r}{\max\limits_j \left(|u_j^n| + \sqrt{Gh_j^n}\right)}, \tag{1.7}$$

where the constant r satisfies $0 < r \le 1$. In our computations, we choose $r = 0.9$. We also enforce zero Neumann boundary conditions for u and h at the artificial boundaries: $u_x = h_x = 0$ for sufficiently large $|x|$.

2. Kinetic schemes

In this section, we will develop a new numerical scheme by extending the existing kinetic flux vector splitting approach. The key idea is to include the source term effect and to well balance the source term and the flow convection.

2.1. The case without source term effect on the flux

To begin with, we consider the shallow water equations without the source term (i.e. $a(x) \equiv 0$):

$$\begin{cases} h_t + (hu)_x = 0, \\ (hu)_t + (hu^2 + \frac{1}{2}Gh^2)_x = 0. \end{cases} \tag{2.1}$$

The (local) Maxwellian distribution for (2.1) is given by

$$g = h\left(\frac{\lambda}{\pi}\right)^{1/2} e^{-\lambda(v-u)^2}, \tag{2.2}$$

where λ is defined by

$$\lambda = \frac{1}{Gh}. \tag{2.3}$$

The connection between the Maxwellian distribution function and the macroscopic flow variables is

$$\begin{pmatrix} h \\ hu \end{pmatrix} = \int_{-\infty}^{\infty} \begin{pmatrix} 1 \\ v \end{pmatrix} g \, dv. \tag{2.4}$$

The fluxes for the corresponding variables are

$$\begin{pmatrix} F_h \\ F_{hu} \end{pmatrix} \equiv \begin{pmatrix} hu \\ hu^2 + \frac{1}{2}Gh^2 \end{pmatrix} = \int_{-\infty}^{\infty} v \begin{pmatrix} 1 \\ v \end{pmatrix} g \, dv. \tag{2.5}$$

We now construct a collisionless Boltzmann scheme by using (2.5) and the kinetic flux–splitting technique. The idea of the construction of the scheme is similar to that used by Pullin [6] who studied the compressible Euler equations. We assume that the initial data $(h_0(x), u_0(x))$ are piecewise constant over the cell $I_j = (x_{j-\frac{1}{2}}, x_{j+\frac{1}{2}})$ (see (1.6)). Let

$$g_j \equiv g(x_j, t, v) = h_j \left(\frac{\lambda_j}{\pi}\right)^{1/2} e^{-\lambda_j (v-u_j)^2}, \tag{2.6}$$

be a Maxwellian distribution in the cell I_j, where $\lambda_j = 1/Gh_j$. For the collisionless scheme, the initial Maxwellian inside each cell is

$$g_0(x) = g_j, \quad x \in I_j, \tag{2.7}$$

where $x = x_{j+1/2}$ is the boundary between cell I_j and I_{j+1}. In the evolution stage, the initial data is propagated according to the collisionless Boltzmann equation, which is

$$g_t + v g_x = 0.$$

The solution of the above equation is

$$g(x_{j+1/2}, t, v) = g_0(x_{j+1/2} - vt) = \begin{cases} g_j, & \text{if } v > 0, \\ g_{j+1}, & \text{if } v < 0. \end{cases} \tag{2.8}$$

Using the formula (2.5), we obtain the numerical fluxes

$$\begin{pmatrix} F_{h,j+1/2} \\ F_{hu,j+1/2} \end{pmatrix} = \int_0^{\infty} \begin{pmatrix} v \\ v^2 \end{pmatrix} g_j \, dv + \int_{-\infty}^{0} \begin{pmatrix} v \\ v^2 \end{pmatrix} g_{j+1} \, dv$$

$$= h_j \begin{pmatrix} \dfrac{u_j}{2}\operatorname{erfc}(-\sqrt{\lambda_j}u_j) + \dfrac{e^{-\lambda_j u_j^2}}{2\sqrt{\pi\lambda_j}} \\ (\dfrac{u_j^2}{2} + \dfrac{1}{4\lambda_j})\operatorname{erfc}(-\sqrt{\lambda_j}u_j) + \dfrac{u_j e^{-\lambda_j u_j^2}}{2\sqrt{\pi\lambda_j}} \end{pmatrix}$$

$$+ h_{j+1} \begin{pmatrix} \dfrac{u_{j+1}}{2}\operatorname{erfc}(\sqrt{\lambda_{j+1}}u_{j+1}) - \dfrac{e^{-\lambda_{j+1} u_{j+1}^2}}{2\sqrt{\pi\lambda_{j+1}}} \\ (\dfrac{u_{j+1}^2}{2} + \dfrac{1}{4\lambda_{j+1}})\operatorname{erfc}(\sqrt{\lambda_{j+1}}u_{j+1}) - \dfrac{u_{j+1} e^{-\lambda_{j+1} u_{j+1}^2}}{2\sqrt{\pi\lambda_{j+1}}} \end{pmatrix} \tag{2.9}$$

where the complementary error function is defined by

$$\mathrm{erfc}(x) = \frac{2}{\sqrt{\pi}} \int_x^\infty e^{-t^2}\ dt.$$

Like sine and cosine functions, $\mathrm{erfc}(x)$, or its double precision $\mathrm{derfc}(x)$, is a given function in FORTRAN and MATLAB.

2.2. The case with source term effect on the flux

In this case, we have a non–zero bottom function $a(x)$. We define the potential function as $\psi(x) = Ga(x)$. Similar to the above discussion, we have at the cell interface $x_{j+1/2}$:

$$g_0(x) = \begin{cases} g_j, & \text{if } x < x_{j+1/2}, \\ g_{j+1}, & \text{if } x > x_{j+1/2}, \end{cases} \quad \text{and } \psi_0(x) = \begin{cases} \psi_j, & \text{if } x < x_{j+1/2}, \\ \psi_{j+1}, & \text{if } x > x_{j+1/2}. \end{cases} \tag{2.10}$$

In order to include the wary bottom effect on the flux, we have to consider two cases.

Case I: $\psi_{j+1} > \psi_j$. In this case, not all of particles with positive velocity v can move to the right cell. The velocity of the particle should be large enough to overcome the potential barrier. In this process, a certain amount of kinetic energy will be transferred into the potential difference $\psi_{j+1} - \psi_j$. The minimum velocity that enables the particle to move from j to $j+1$ is

$$\frac{1}{2}\tilde{v}_j^2 = \psi_{j+1} - \psi_j, \quad \text{or } \tilde{v}_j = \sqrt{2(\psi_{j+1} - \psi_j)}. \tag{2.11}$$

The numerical mass flux is then given by

$$\begin{aligned} F_{h,j+1/2} &= \int_{\tilde{v}_j}^\infty v g_j\ dv + \int_{-\infty}^0 v g_{j+1}\ dv \\ &= \frac{h_j u_j}{2}\mathrm{erfc}\left(\sqrt{\lambda_j}(\tilde{v}_j - u_j)\right) + \frac{h_j}{2\sqrt{\pi\lambda_j}} e^{-\lambda_j(\tilde{v}_j - u_j)^2} \\ &\quad + \frac{h_{j+1}u_{j+1}}{2}\mathrm{erfc}(\sqrt{\lambda_{j+1}}u_{j+1}) - \frac{h_{j+1}}{2\sqrt{\pi\lambda_{j+1}}} e^{-\lambda_{j+1}u_{j+1}^2}. \end{aligned} \tag{2.12}$$

If we introduce the following notations

$$F_{hu,j+1/2}^L = \int_{\tilde{v}_j}^\infty v^2 g_j\ dv = \int_0^\infty v^2 g_j\ dv - F_{hu,j+1/2}^*, \tag{2.13}$$

$$F_{hu,j+1/2}^* = \int_0^{\tilde{v}_j} v^2 g_j\ dv, \tag{2.14}$$

$$F_{hu,j+1/2}^R = \int_{-\infty}^0 v^2 g_{j+1}\ dv, \tag{2.15}$$

then the momentum flux is taken as

$$F_{hu,j+1/2} = F^L_{hu,j+1/2} + F^R_{hu,j+1/2}. \tag{2.16}$$

By using the definition (2.6) for g_j, we can find the explicit form for the integral (2.14):

$$F^*_{hu,j+1/2} = \left(\frac{h_j}{4\lambda_j} + \frac{h_j u_j^2}{2}\right)\left[\mathrm{erfc}\Big(-\sqrt{\lambda_j}u_j\Big) - \mathrm{erfc}\Big(\sqrt{\lambda_j}(\tilde{v}_j - u_j)\Big)\right]$$

$$+\frac{h_j u_j}{2\sqrt{\lambda_j \pi}}\left[e^{-\lambda_j u_j^2} - e^{-\lambda_j(\tilde{v}_j - u_j)^2}\right] - \frac{h_j \tilde{v}_j}{2\sqrt{\lambda_j \pi}} e^{-\lambda_j(\tilde{v}_j - u_j)^2}. \tag{2.17}$$

The explicit forms of the integrals in (2.13) and (2.15) have been given in (2.9).

Case II: $\psi_{j+1} < \psi_j$. Similarly, we define in this case

$$\tilde{v}_j = \sqrt{2(\psi_j - \psi_{j+1})}. \tag{2.18}$$

The numerical mass flux is given by

$$F_{h,j+1/2} = \int_0^\infty v g_j \, dv + \int_{-\infty}^{-\tilde{v}_j} v g_{j+1} \, dv$$

$$= \frac{h_j u_j}{2}\mathrm{erfc}(\sqrt{\lambda_j}u_j) + \frac{h_j}{2\sqrt{\pi\lambda_j}} e^{-\lambda_j u_j^2} + \frac{h_{j+1}u_{j+1}}{2}\mathrm{erfc}\left(\sqrt{\lambda_{j+1}}(\tilde{v}_j + u_{j+1})\right)$$

$$- \frac{h_{j+1}}{2\sqrt{\pi\lambda_{j+1}}} e^{-\lambda_{j+1}(\tilde{v}_j + u_{j+1})^2}, \tag{2.19}$$

and the momentum flux is

$$F_{hu,j+1/2} = F^L_{hu,j+1/2} + F^R_{hu,j+1/2}, \tag{2.20}$$

where

$$F^L_{hu,j+1/2} = \int_0^\infty v^2 g_j \, dv, \tag{2.21}$$

$$F^R_{hu,j+1/2} = \int_{-\infty}^{-\tilde{v}_j} v^2 g_{j+1} \, dv := \int_{-\infty}^{0} v^2 g_{j+1} \, dv - F^*_{hu,j+1/2}. \tag{2.22}$$

It is noted that all integrals in (2.21) and (2.22) can be expressed by the complementary error functions. In particular, we have

$$F^*_{hu,j+1/2} = \int_{-\tilde{v}_j}^{0} v^2 g_{j+1} \, dv = \left(\frac{h_{j+1}}{4\lambda_{j+1}} + \frac{h_{j+1}u_{j+1}^2}{2}\right)\left[\mathrm{erfc}\Big(\sqrt{\lambda_{j+1}}u_{j+1}\Big)\right.$$

$$\left.-\mathrm{erfc}\Big(\sqrt{\lambda_{j+1}}(\tilde{v}_j + u_{j+1})\Big)\right] - \frac{h_{j+1}u_{j+1}}{2\sqrt{\lambda_{j+1}\pi}}\left[e^{-\lambda_{j+1}u_{j+1}^2} - e^{-\lambda_{j+1}(\tilde{v}_j + u_{j+1})^2}\right]$$

$$- \frac{h_{j+1}\tilde{v}_j}{2\sqrt{\lambda_{j+1}\pi}} e^{-\lambda_{j+1}(\tilde{v}_j + u_{j+1})^2}. \tag{2.23}$$

To conclude this section, the shallow water equations (1.1) will be solved by the following schemes:

$$\begin{cases} h_j^{n+1} = h_j^n + \dfrac{\Delta t_n}{\Delta x}(F_{h,j-1/2}^n - F_{h,j+1/2}^n), \\ (hu)_j^{n+1} = (hu)_j^n + \dfrac{\Delta t_n}{\Delta x}(F_{hu,j-1/2}^n - F_{hu,j+1/2}^n) - \Delta t_n G a'(x_j) h_j^{n+1}. \end{cases} \tag{2.24}$$

Our proposed gas-kinetic method is the scheme (2.24) with the fluxes (2.12),(2.16), (2.19) and (2.20). On the other hand, the KFVS scheme refers to the scheme (2.24) with flux (2.9).

Note that the scheme (2.24) is of semi–implicit type, which is similar to the LxF scheme (1.5). The only difference for the schemes tested in this paper is about how to evaluate the flux functions in the above equations at a cell interface.

3. Positivity–preserving analysis

For physical problems, some physical variables such as density and height of the water should be able to preserve these positivity requirements. In the following, we show that the water height h computed by the gas–kinetic scheme (2.24) is always non–negative. The analysis is similar to an earlier work by Tang and Xu [8], where the positivity-preserving analysis is made for the gas-kinetic schemes for the compressible Euler equations.

To begin with, we first consider the case with flat bottom.

Lemma 3.1. *If $\{h_j^n\}$ is non–negative, then $\{h_j^{n+1}\}$ is also non–negative provided the CFL condition (1.7) is satisfied. Here $\{h_j^{n+1}\}$ is the solution of the scheme (2.24) with numerical flux (2.9).*

Proof. The equation (2.24) with numerical flux (2.9) can be written as

$$h_j^{n+1} = A_1 h_{j-1}^n + A_2 h_j^n + A_3 h_{j+1}^n, \tag{3.1}$$

where

$$A_1 = \sigma \int_0^\infty v \left(\frac{\lambda_{j-1}}{\pi}\right)^{1/2} e^{-\lambda_{j-1}(v-u_{j-1})^2}\, dv,$$

$$A_2 = 1 - \sigma \int_{-\infty}^\infty |v| \left(\frac{\lambda_j}{\pi}\right)^{1/2} e^{-\lambda_j(v-u_j)^2}\, dv,$$

$$A_3 = -\sigma \int_{-\infty}^0 v \left(\frac{\lambda_{j+1}}{\pi}\right)^{1/2} e^{-\lambda_{j+1}(v-u_{j+1})^2}\, dv.$$

Here $\sigma = \Delta t_n/\Delta x$.

It is obvious that $A_1 \geq 0$ and $A_3 \geq 0$. Next we show that A_2 is also non–negative under the CFL condition (1.7). Actually, we have

$$A_2 = 1 - \frac{\sigma}{2}\left[\left(u_j \mathrm{erfc}(-\sqrt{\lambda_j}u_j) + \frac{e^{-\lambda_j u_j^2}}{\sqrt{\lambda_j \pi}}\right) - \left(u_j \mathrm{erfc}(\sqrt{\lambda_j}u_j) - \frac{e^{-\lambda_j u_j^2}}{\sqrt{\lambda_j \pi}}\right)\right]$$

$$= 1 - \frac{\sigma}{\sqrt{\lambda_j}}\left[\beta_j - \beta_j \mathrm{erfc}(\beta_j) + \frac{1}{\sqrt{\pi}} e^{-\beta_j^2}\right], \tag{3.2}$$

where $\beta_j = \sqrt{\lambda_j}u_j$, and we have used the identity $\mathrm{erfc}(x) + \mathrm{erfc}(-x) = 2$.

For convenience, we will omit subscript j in the following. Let $Y(\beta) := \beta - \beta \mathrm{erfc}(\beta) + \frac{1}{\sqrt{\pi}} e^{-\beta^2}$. If we have

$$\frac{Y(\beta)}{\sqrt{\lambda}} \leq \frac{|\beta| + 1}{\sqrt{\lambda}} \equiv |u| + \sqrt{Gh}, \tag{3.3}$$

then it can be shown that the coefficient A_2 is non–negative under the CFL condition (1.7), which will complete the proof of this lemma. The remaining task is to verify the inequality (3.3), i.e.

$$|\beta| + 1 \geq Y(\beta),$$

or equivalently

$$Z(\beta) := |\beta| + 1 - Y(\beta) \geq 0.$$

Three cases will be considered.

- (i) If $\beta = 0$, then we have $Z(\beta) = 1 - \frac{1}{\sqrt{\pi}} > 0$.
- (ii) If $\beta \in (0, \infty)$, then $Z(\beta)$ can be represented as

$$Z(\beta) = 1 + \beta \mathrm{erfc}(\beta) - \frac{1}{\sqrt{\pi}} e^{-\beta^2}.$$

  It follows from $Z'(\beta) = \mathrm{erfc}(\beta) \geq 0$ and $Z(0) > 0$ that $Z(\beta) \geq 0$ for all $\beta > 0$.
- (iii) If $\beta \in (-\infty, 0)$, then $Z(\beta)$ becomes

$$Z(\beta) = -2\beta + 1 + \beta \mathrm{erfc}(\beta) - \frac{1}{\sqrt{\pi}} e^{-\beta^2}.$$

  In this case, we have $Z'(\beta) = -2 + \mathrm{erfc}(\beta) \leq 0$. This result, together with $Z(0) > 0$, implies that $Z(\beta)$ is also positive for $\beta \in (-\infty, 0)$.

Therefore, the proof of this lemma is complete.

We can easily extend the results in **Lemma** 3.1 to the non–flat bottom case.

Lemma 3.2. *If $\{h_j^n\}$ is non–negative, then $\{h_j^{n+1}\}$ is also non–negative provided that the CFL condition (1.7) is satisfied. Here $\{h_j^{n+1}\}$ is the solution of (2.24) with numerical flux (2.12) or (2.19).*

Proof. The first equation of (2.24) can be written as

$$h_j^{n+1} = \overline{A}_1 h_{j-1}^n + \overline{A}_2 h_j^n + \overline{A}_3 h_{j+1}^n, \tag{3.4}$$

where

$$\overline{A}_1 = \sigma \int_{\alpha_1}^{\infty} v \left(\frac{\lambda_{j-1}}{\pi}\right)^{1/2} e^{-\lambda_{j-1}(v-u_{j-1})^2}\, dv,$$

$$\overline{A}_2 = 1 - \sigma \int_{\alpha_1}^{\infty} v \left(\frac{\lambda_j}{\pi}\right)^{1/2} e^{-\lambda_j(v-u_j)^2}\, dv + \sigma \int_{-\infty}^{-\alpha_2} v \left(\frac{\lambda_j}{\pi}\right)^{1/2} e^{-\lambda_j(v-u_j)^2}\, dv,$$

$$\overline{A}_3 = -\sigma \int_{-\infty}^{-\alpha_2} v \left(\frac{\lambda_{j+1}}{\pi}\right)^{1/2} e^{-\lambda_{j+1}(v-u_{j+1})^2}\, dv.$$

Here $\alpha_1 = 0$ or v_j with $v_j = \sqrt{2(\psi_{j+1} - \psi_j)}$, and $\alpha_2 = 0$ or $-v_{j-1}$ with $v_{j-1} = \sqrt{2(\psi_{j-1} - \psi_j)}$. It is obvious that $\overline{A}_2 \geq A_2$. Thus under the CFL condition (1.7), $\overline{A}_2 \geq 0$. Similarly, we also have $\overline{A}_1 \geq 0$ and $\overline{A}_3 \geq 0$. Therefore h_j^{n+1} is non–negative, under the assumption of this lemma.

4. Numerical experiments

In this section, we present several numerical examples to test our gas–kinetic scheme (2.24) with numerical flux (2.12) and (2.16) or (2.19) and (2.20) for the shallow water equations with the source term. For comparison, numerical results of the LxF scheme (1.5) and the conventional KFVS scheme (2.24) with numerical flux (2.9) will be also included. In solving the hyperbolic conservation laws with stiff source terms, the LxF scheme was employed by Chalabi and Qiu [2] also for comparison purpose and it was observed that the LxF scheme provides shock locations incorrectly.

In the first two examples, we consider the following $a(x)$:

$$a(x) = \begin{cases} 0.3\Big(\cos\big(\pi(x-1)/2\big)\Big)^{30}, & |x-1| \leq 1, \\ 0, & \text{otherwise.} \end{cases} \tag{4.1}$$

This bottom function is similar to that used in [3].

Example 4.1. *Consider the equation (1.1) with the wavy bottom function (4.1) and the initial condition*

$$(h_0(x), u_0(x)) = (1 - a(x), 1). \tag{4.2}$$

The initial data indicates that the initial total height is 1 and the initial velocity is 1 everywhere. The computational domain used is $(-1, 3)$. For this example, the equilibria governed by (1.2) and (1.3) exists and can be computed by MATLAB (see solid lines in Figs. 2 (a)-(b).)

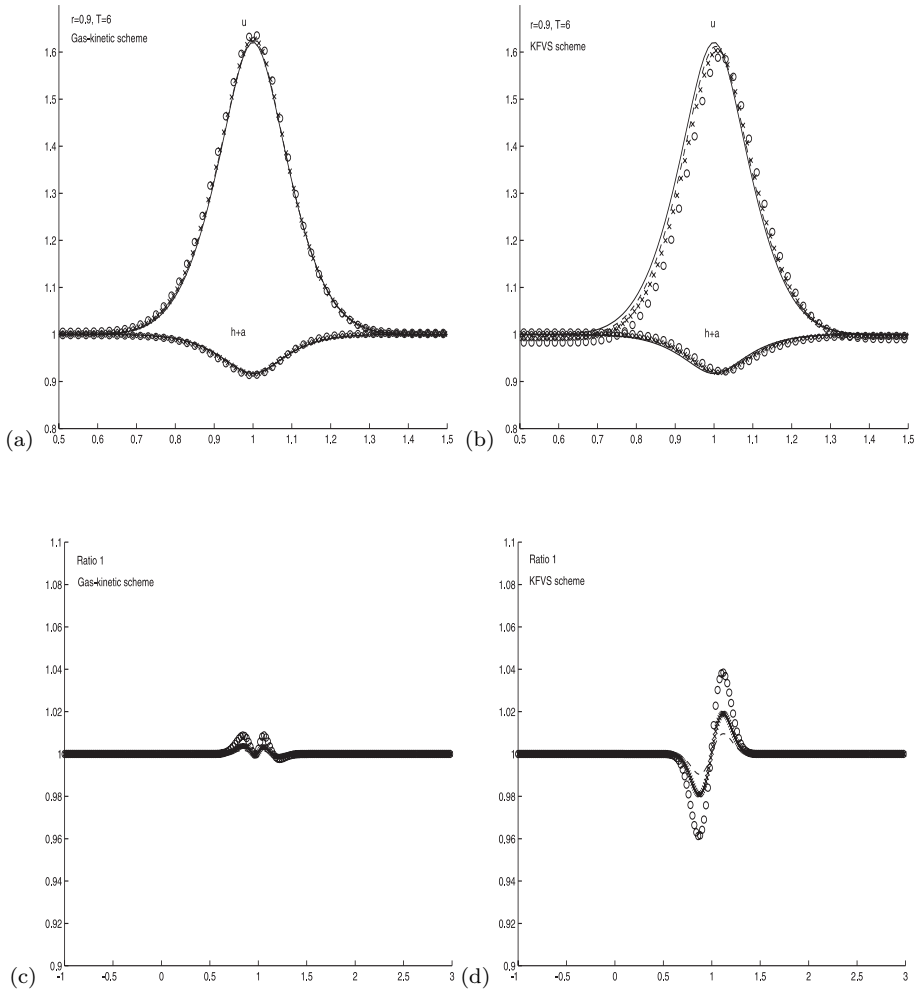

Figure 2. Example 4.1: (a) Top solid curve is the exact solution for u and bottom solid curve is for $h + a$, and numerical results are obtained by using the proposed gas-kinetic scheme; (b) Same as (a) except by using the traditional KFVS scheme; (c) Ratio (4.3) obtained by using the proposed gas-kinetic scheme; (d) Ratio (4.3) obtained by using the KFVS scheme. The mesh sizes used are $\Delta x = \frac{1}{50}$ ('o'), $\frac{1}{100}$ ('x'), and $\frac{1}{200}$ (dashed line).

The results obtained by using the gas-kinetic method proposed in this work and the conventional KFVS scheme with the mesh-refinement are shown in Fig. 2. The output data are $h + a$ and the fluid velocity u at $t = 6$, which are compared with the exact solution (solid line). Since $t = 6$ is large enough, we can consider that the flow almost reaches steady state at this time. From Figs. 2 (a)

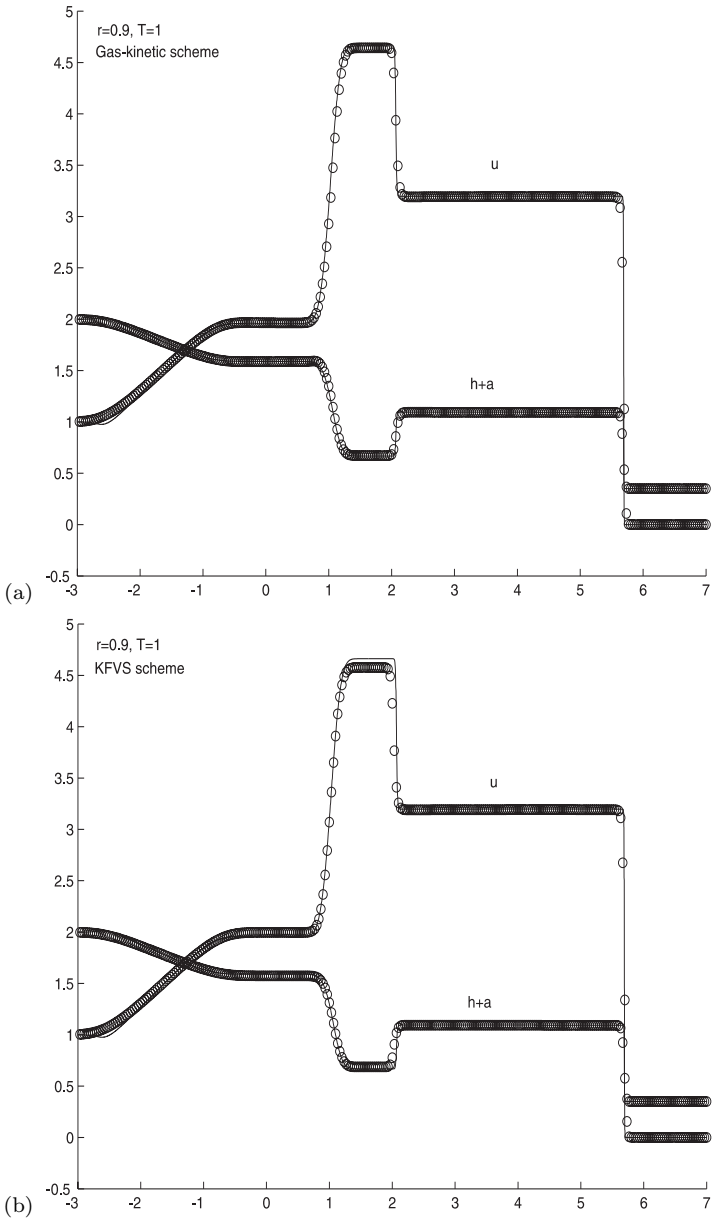

Figure 3. Example 4.2: (a) Exact solutions (solid line) and numerical solutions obtained by using the gas-kinetic scheme with $\Delta x = \frac{1}{30}$ ("$\diamond$"); (b) Same as (a) except that by using the KFVS scheme.

and (b), we can see that the gas-kinetic method has much less phase error than the conventional KFVS scheme. We also plot in Figs. 2 (c) and (d) the following ratio:

$$\mathsf{ratio}(x,t) = \frac{h(x)u(x,t)}{h_- u_-}. \tag{4.3}$$

It follows from (1.2) that this ratio should equal to 1 at steady state. The mesh–refinement analysis in Fig. 2 for the above ratio indicates that the proposed gas–kinetic scheme is more appropriate than the KFVS scheme in preserving the unit ratio.

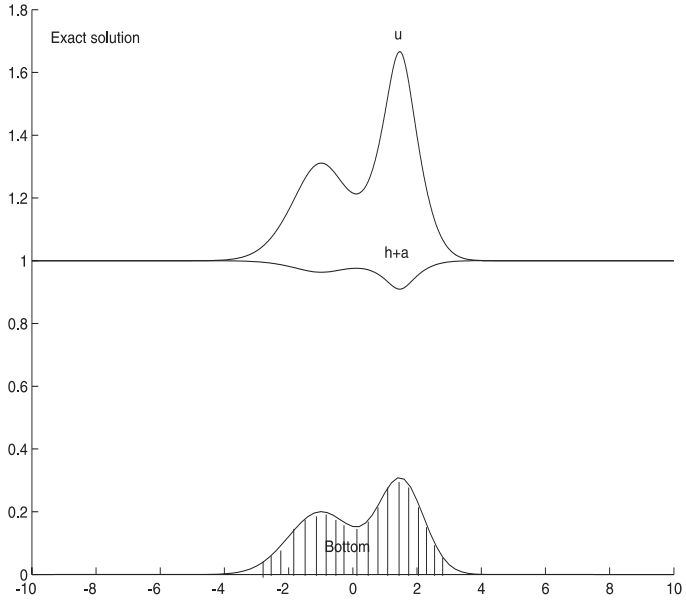

Figure 4. Equilibrium for Example 4.3.

Example 4.2. *Consider the equation (1.1) with the wavy bottom function (4.1) and the initial condition*

$$(h_0(x), u_0(x)) = \begin{cases} (2 - a(x), 1), & x < 1, \\ (0.35 - a(x), 0), & x \geq 1. \end{cases} \tag{4.4}$$

This is an unsteady flow calculation. The computational domain used is $(-10, 10)$. In order to have a close look at the solution around the wary bottom, we present the numerical solutions in part of the computational domain $-3 \leq x \leq 7$. The results from the gas-kinetic method and the KFVS scheme are shown in Fig. 3, where the mesh size used is $\Delta x = \frac{1}{30}$. The solid line shows the

solution obtained using the LxF scheme with $\Delta x = \frac{1}{500}$. It is observed that the numerical result with the gas-kinetic scheme is slightly more accurate than that with the KFVS scheme, in particular for the solution of the velocity u.

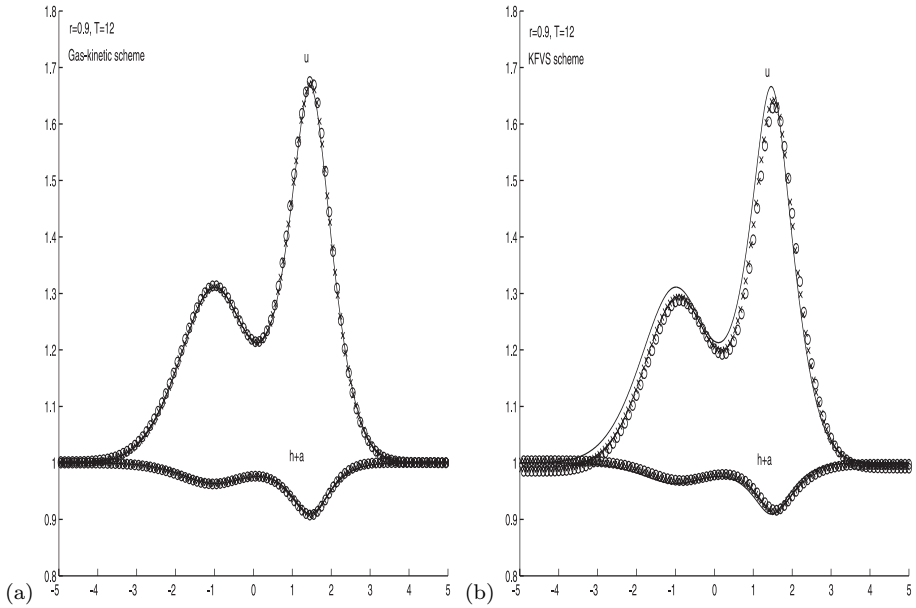

(a) (b)

Figure 5. Exact solution (solid line) and the numerical solutions for Example 4.3. Numerical solutions are obtained by using (a): the gas–kinetic scheme proposed in this work and (b): the traditional KFVS scheme, with $\Delta x = \frac{1}{10}$ ('o') and $\frac{1}{15}$ ('x').

Example 4.3. *This is also a steady state calculation with the initial condition (4.2). The bottom shape is changed to*

$$a(x) = 0.2e^{-(x+1)^2/2} + 0.3e^{-(x-1.5)^2}. \tag{4.5}$$

The computational domain is $(-10, 10)$, and the left boundary condition is $u_- = 1$ and $h_- = 1$. The equilibria solution can be obtained exactly for this problem, see Fig. 4. The numerical solutions for the fluid velocity and the total height are shown in Fig. 5. Again, the advantage of the proposed gas-kinetic scheme is demonstrated, due to the inclusion of the source term effect in a flux evaluation.

Example 4.4. *We consider a problem same as Example 4.3, except that the initial fluid flow is assumed to be at rest.*

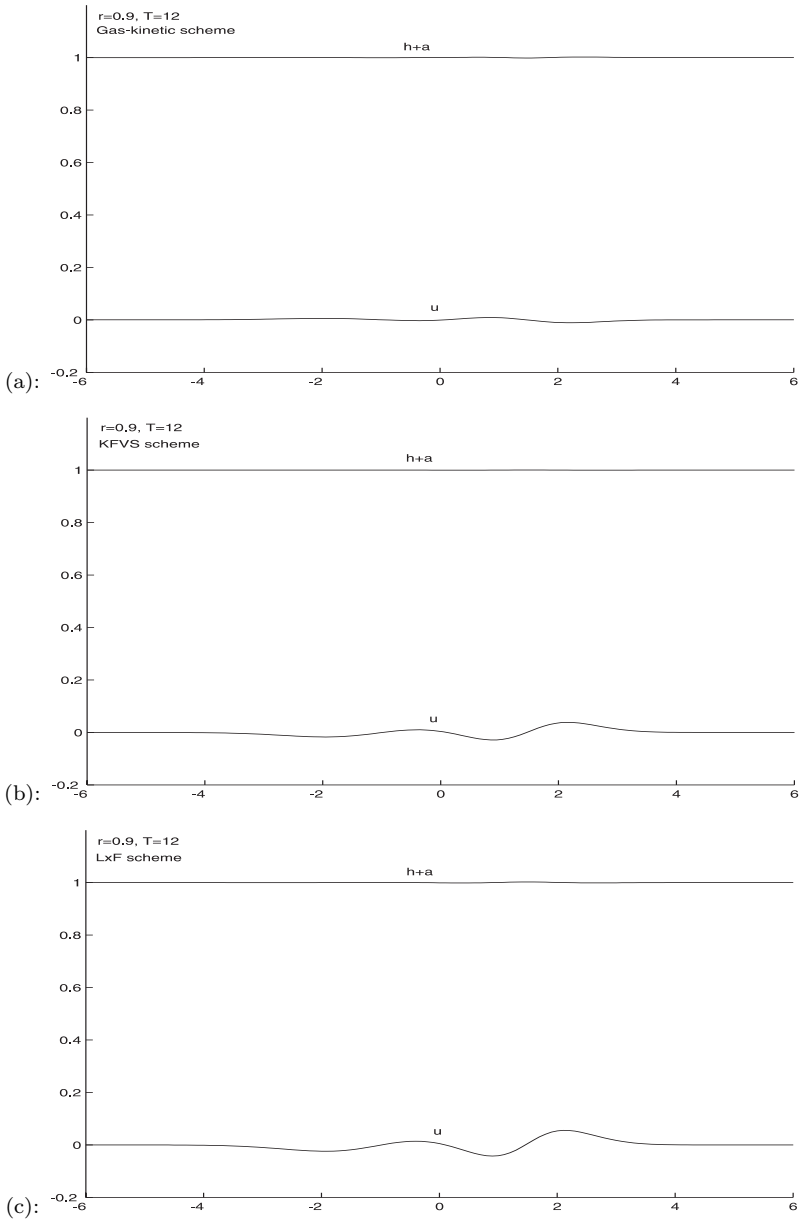

Figure 6. Example 4.4: The numerical solutions (solid lines) are obtained by using (a): the gas-kinetic scheme, (b) the KFVS scheme, (c) the LxF scheme, with $\Delta x = \frac{1}{10}$.

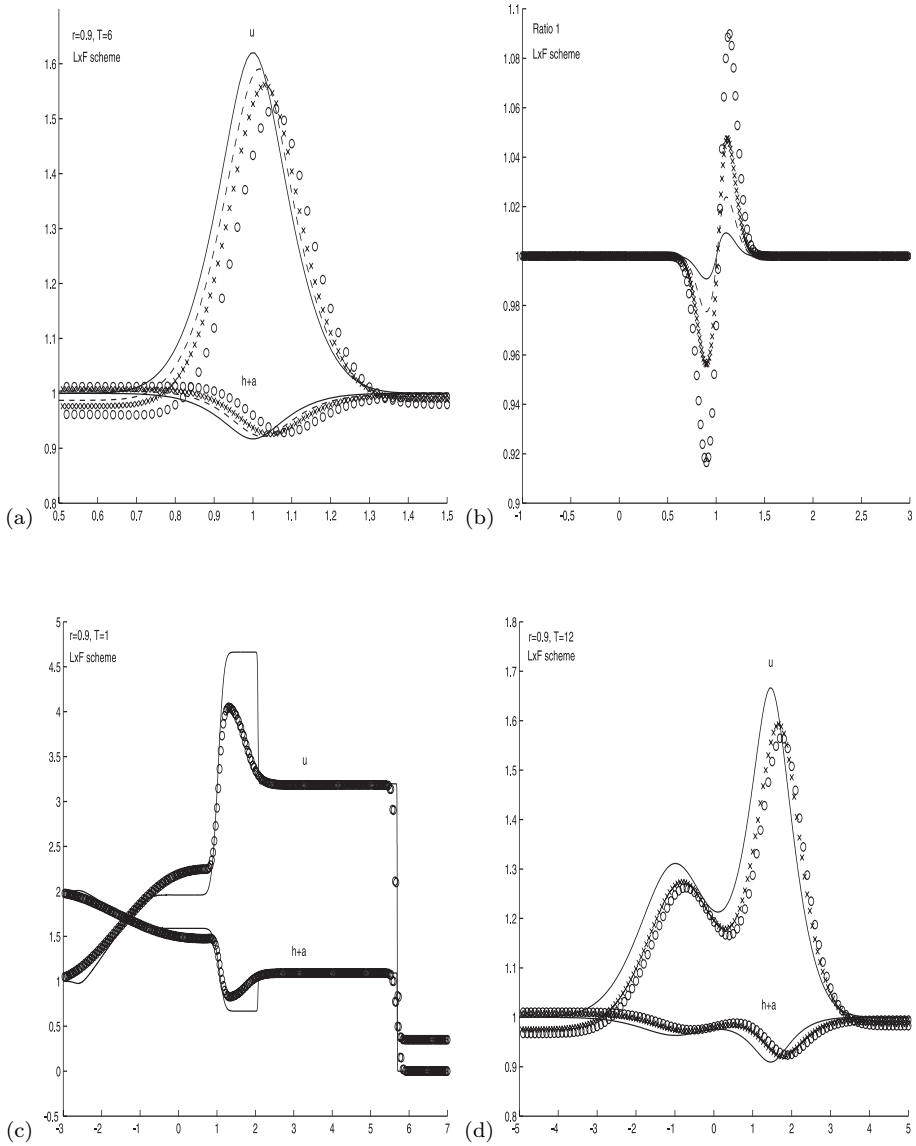

Figure 7. Except with the use of the LxF scheme, the above figures are (a): same as Fig. 2 (a); (b): same as Fig. 2 (c); (c): same as Fig. 3 (a); and (d): same as Fig. 5 (a).

This problem is also considered by Jin [4]. The steady state solutions obtained by using the gas-kinetic scheme, the KFVS scheme and the LxF scheme are shown in Fig. 6. All three schemes can obtain the correct steady state solution for $h+a$, but only the gas-kinetic method gives the most accurate approximation to the exact solution $u=0$.

Finally, we plot in Fig. 7 the performance of the LxF scheme to Examples 4.1–4.3. The numerical experiments indicate that the LxF scheme requires much smaller mesh size than that for the gas-kinetic scheme in order to obtain the same solution resolution.

5. Conclusions

In this paper, the gas-kinetic flux vector splitting scheme is extended to solving the shallow water equations with source term. Due to the inclusion of the source term effect on the flux evaluation across cell interfaces, the proposed kinetic method preserves the equilibria better than the conventional KFVS scheme. Moreover, the positivity of the proposed kinetic scheme, which preserves the non-negative water height, is established.

Acknowledgments

The research of HZT is partially supported by the National Natural Science Foundation of China (No. 19901031), the Special Funds for Major State Basic Research Projects of China, and Alexander von Humboldt Foundation. The research of TT and KX is partially supported by RGC Grants of Hong Kong Research Grants Council.

References

[1] A. Berbudez and M. E. Vazquez, Upwind methods for hyperbolic conservation laws with source terms, *Computers & Fluids* **23** (1994), 1049–1071.
[2] A. Chalabi and Y. Qiu, Relaxation schemes for hyperbolic conservation laws with stiff source terms: Application to reacting Euler equations, *J. Sci. Comp.* **15** (2000), 395-416.
[3] J.M. Greenberg and A.Y. LeRoux, A well–balanced scheme for the numerical processing of source terms in hyperbolic equations, *SIAM J. Numer. Anal.* **33**(1996), 1–16.
[4] S. Jin, A steady-state capturing method for hyperbolic system with geometrical source terms, *Math. Model. Anal.* **35** (2001), 631–646.
[5] R.J. LeVeque, Balancing source terms and flux gradients in high-resolution Godunov methods: the quasi-steady wave-propagation algorithm, *J. Comput. Phys.* **146** (1998), 346–365.
[6] D. I. Pullin, Direct simulations methods for compressible inviscid ideal gas–flows, *J. Comput. Phys.* **34** (1980), 231–244.
[7] P. L. Roe, Upwind difference schemes for hyperbolic conservation laws with source terms, *Proc. Conference Hyperbolic Problems*, eds. Carasso, Raviart and Serre, Springer, pp. 41–51 (1986).

[8] T. Tang and K. Xu, Gas-kinetic schemes for the compressible Euler equations: positivity-preserving analysis, *ZAMP* **50** (1999), 258-281.
[9] M. E. Vazquez-Cendon, Improved treatment of source terms in upwind schemes for shallow water equations in channels with irregular geometry, *J. Comput. Phys.* **148** (1999), 497–526.
[10] K. Xu, A gas–kinetic scheme for the Euler equations with heat transfer, *SIAM J. Sci. Comput.* **20** (1999), 1317–1335.

Huazhong Tang
LMAM & School of Mathematical Sciences
Peking University
Beijing 100871
China
e-mail: htang@math.pku.edu.cn

Tao Tang
Department of Mathematics
Hong Kong Baptist University
Kowloon Tong
Hong Kong
e-mail: ttang@math.hkbu.edu.hk

Kun Xu
Department of Mathematics
Hong Kong University of Science and Technology
Clear Water Bay
Hong Kong
e-mail: makxu@ust.hk

(Received: October 24, 2001)